MARGIN SETTING ALGORITHM FOR MAMMOGRAM SEGMENTATION AND REGISTRATION

Huda Al-Ghaib[1], Yi Wang[1], and Reza Adhami[1]
[1]Electircal and Computer Engineering, the University of Alabama in Huntsville, Huntsville City, Alabama 35900

ABSTRACT
A machine learning algorithm entitled margin setting algorithm (MSA), for mammogram segmentation is presented. MSA uses hyperspheres to classify nonlinear patterns in mammograms to their corresponding classes. In this paper, we used MSA to segment the breast object in mammograms. The segmented mammograms are inputted to a mutual information (MI) algorithm for mammogram registration. MSA performance is compared with neural network (NN) and several thresholding techniques. For the registration outcomes, signal to noise ratio (SNR) and correlation (CORR) metrics are computed to evaluate the performance of the registration algorithms. It is shown that the mammogram registration using MSA segmentation delivers (0.22%, 1.63%) increase in (SNR, CORR) compared with the NN. However, when compared with the thresholding techniques, MSA delivers a significant improvement in (SNR, CORR) values.

KEYWORDS: *Margin setting algorithm, neural network, thresholding, mutual information, segmentation, and registration.*

I. INTRODUCTION

Image registration is used when two images are being compared against each other. For this reason, registration has wide applications that may vary from computer vision to medical diagnosis [1]-[2]. Computer vision applications include tasks such as video tracking motion, pattern detection, 3-D information extraction, and remote sensing image reconstruction [3]. Medical applications of registration include population modeling and statistical atlases, longitudinal studies, and multi-modality fusion. Population modeling and statistical atlases characterizes the normal pattern of an organ. Longitudinal studies examine the changes in lesion's shape over time in temporal images for the purpose of monitoring and studying different diseases. Temporal images are defined as images obtained using the same device at different time frames, months or even years. Multi-modality fuses images acquired from different sensors [4]-[6].

One example of the medical modalities that uses registration process is mammography. Mammogram registration attempts to find the difference in temporal mammograms that may correspond to the presence of carcinoma. Some of these cells are slow growing and gradually form a lesion causing a small architectural distortion. Hence, they may go undetected by a radiologist when he or she visually compares the patient temporal mammograms. An automated mammograms registration that could pinpoint these changes may increase the chance of detecting abnormalities in their early stages by radiologists [23]. It has been noted that early detection of breast cancer increases the survival rates and provides better treatment options [7], [24]. Figure 1 illustrates a temporal case for one patient acquired on May 23, 2012 and June 6, 2013, respectively, with architectural distortion shown as tent region behind the nipple. The mammogram shown in Figure 1. a) is known as the reference mammogram while the one in Figure 1. b) is the target mammogram. When the reference and target mammograms are visually compared by the radiologist she was only concerned about the area behind the nipple. The area highlighted by the rectangle did not need extra investigations. Figure 1. c) shows the result of registering the reference and target mammograms using mutual information (MI). The target image is transformed to have similar rotation, scale, and translation of the reference

mammogram [25]. Figure 1. c) directed the radiologist's attention to multi-focal areas that are corresponding to malignant lesions. The multi-focal areas are highlighted by rectangles in Figure 1. c).

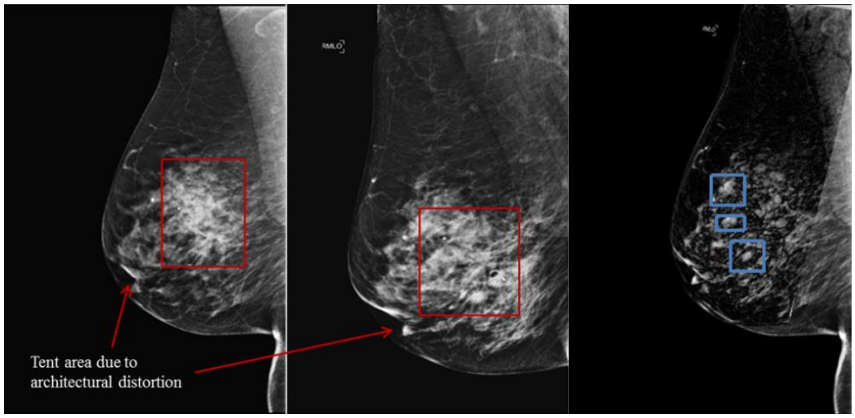

Figure 1. Temporal case with a) reference, b) target, and c) superimposed registered mammograms

Automated mammogram registration is a challenging task due to internal and external factors. Internal factors are related to changes in the breast characteristics with time. For instance, the tissues in female breasts change with the hormonal level and age. External factors include the positioning and the use of different facilities during the imaging process. Unfortunately, the exact positioning of two consecutive mammograms is not possible. Also, lesions that are three dimensional are projected onto two dimensional images. Any small rotation in the breast during the imaging process may hide the lesion in one of the images and affect the registration process. Figure 2. demonstrates the reference and target mammograms for one patient acquired on May 24, 2012 and May 23, 2013, respectively.

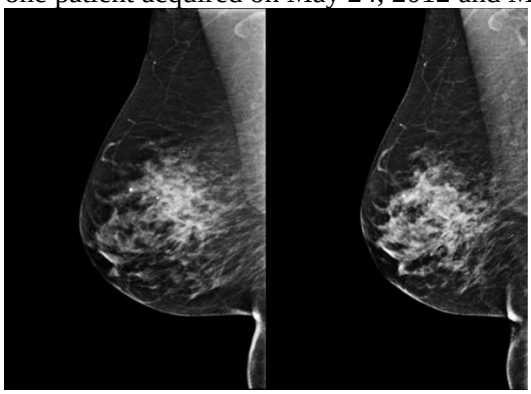

Figure 2. Temporal case with a) reference and b) target mammograms

Figure 3. a) illustrates the superimposed registered reference and target mammograms shown in Figure2. Figure 3. b) provides the difference between the two registered mammograms in Figure 3. a). The registration in Figure 3 a) is not exact and the internal information for the target mammogram is shifted to the right, i.e., highlighted by an arrow in Figure 3. a). Image subtraction in Figure 3. b) delivers blurry image with numerous black curves that are highlighted by arrows. In this case, inexact registration provided no meaningful information to the radiologist.

The current registration algorithms need further improvement to provide meaningful information to radiologists. A preprocessing step of mammogram landmark segmentation could increase the accuracy of registration step. Segmentation extracts an object of interest from the background. Thresholding is one of the simplest segmentation algorithms. It uses the histogram information to compute a threshold value that separates the object from the background [8]. Medical images include objects that are not well separable from the background. In this case, thresholding fails to provide desirable results. To overcome the shortcoming of the thresholding technique we use a machine learning algorithm. A machine learning algorithm consists of two phases; learning and classification. The learning phase uses a set of input patterns with a known class (training dataset). In this phase, features such as length, shape, color, or intensity values, are extracted from each pattern. In these algorithms, only the features that classify the patterns to their classes are selected. These features

provide a decision boundary separating the classes. The decision boundaries are utilized in the classification phase to classify the testing input sets to their classes. When a machine learning algorithm is designed to segment an object in a grayscale image, the input features are the intensity values and the output classes are the object and background. Unlike Support vector machine (SVM) and neural network (NN), a relatively new machine learning algorithm, called margin setting algorithm (MSA) uses prototypes to determine the decision boundaries that classify objects into their classes [9]-[12]. MSA appears to provide better results for classifying nonlinear patterns compared with other machine learning algorithms such as SVM and NN [13]-[14]. MSA has been used in applications such as artificial colors segmentation, noise estimation, and hyperspectral [15]-[16]. Recently, a Fourier-based MSA was proposed to recognize the shape, size, pose, and location of a target in a scene [12].

In this paper, we designed, implemented, and evaluated the performance of MSA for breast segmentation in mammograms. MSA algorithm is compared with NN and several thresholding techniques; global, ant colony optimization (ACO), and Otsu [22]. The output of the MSA is used an input to mutual information (MI) algorithm for registration. MI uses statistical information to compute the optimal rotation, scale, and translation that maps two images [20]-[21]. The mathematical representation for MSA and object classification algorithm using MSA are explained in section II. The dataset used in this research are also presented in the DESIGN and MMTERIAL section. The segmentation methodology, segmentation evaluation, registration methodology, and registration evaluation are given in the PROCEDURE, RESULTS, AND DISCUSSION section. The conclusions and future works are given in sections four and five, respectively.

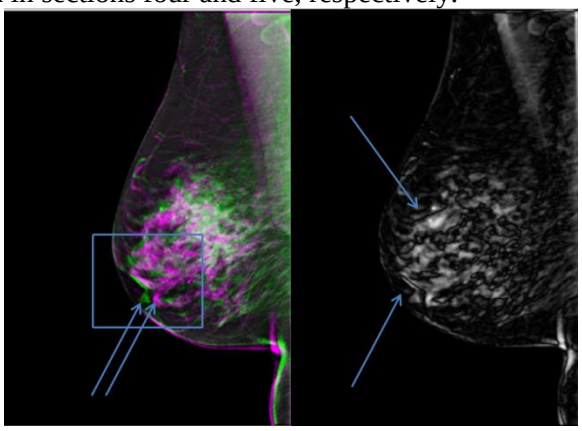

Figure 3. a) Registered pair mammograms, and b) image difference for a)

II. DESIGN AND MATERIAL

2.1. Margin Setting Algorithm

Statistical pattern recognition algorithms classify an object into its appropriate classes based on learned hypotheses. The learned hypotheses are concluded from a set of training data to illustrate generalization for a classification problem. In order to obtain a desirable classifier, generalization has to be of high confidence. The high confidence requirement is only true when the data of different classes are well separable using a decision surface boundary. In this case, the margin between the decision boundary and the nearby points is maximized. In SVM, these points are known as the support vectors. For 2-class problem, a decision boundary with maximized margin for the support vectors is easily computed. Increasing the problem dimensionality increases the algorithm and generalization complexity. To overcome this obstacle, an alternative approach is proposed through Boosting algorithm [9]. Boosting subdivides the training set into a number of subsets. A classifier is then trained for each subset. Each classifier provides a poor performance known as a weak classifier. The weak classifiers could be combined using different weights to produce a strong classifier. Strong classifier has small misclassification rate only when the appropriate weights are selected. In general, weights are not always easy to calculate. Margin setting algorithm (MSA) is introduced to overcome the shortcomings of the SVM and Boosting algorithms. Elements from both algorithms are combined in MSA to demonstrate good generalization without complicating the decision. These elements

include dimensionality and decision surface from SVM and dividing the training set into subsets from Boosting. Thus, each subset is classified using a separate decision surface. Final decision is reached by combining the decisions from the various classifiers using a non-linear approach.

2.2. Object Classification using MSA

The flowchart given in Figure 4. is applied to segment the breast in mammograms. The steps involved in the algorithm can be summarized as:

Step 1, **Construction of the training set:** Select M random points from the test image to construct the training set $t = \{x_i, \text{ for } i = 1 \text{ to } M\}$. t is a 1-D vector with intensity values that are corresponding to both object and background classes.

Step 2, Subdivision of training set: partition process is applied to subdivide the original training set, *S*, into number of subsets as:

$$S = \bigcup_{i>1} S_i \tag{1}$$

where $S_i \bigcap S_j = \varnothing$ for $i \neq j$.

Step 3, **Construction of initial prototypes:** Create the initial prototypes, for each subset, within the training set intensity range and using normal distribution. The initial prototypes are represented mathematically as:

$$G = \{(\delta_k, r_k, \eta_m),\ 1 \le k \le M,\ 1 \le m \le P\} \tag{2}$$

δ_k and r_k are the center and radius of G, respectively, η_m is the class label with P total number of classes, and *M* is the number of prototypes that belong to class η_m. In the beginning, *N* random points are selected as initial prototypes.

Step 4, Select potential prototypes from initial prototypes: Examine each prototype to select the potential prototypes of minimum Euclidean distance to the object points and of maximized zero-margin radius. Zero-margin is defined as the distance from the center of the prototype to the closest non-class point.

Step 5, Select final prototype for current mutation: Compute the figure of merit for each potential prototype. Figure of merit is defined as the number of points from the class set around a potential prototype that are within the zero-margin radius. Figure of merit is a measurement of true positive rate for a given prototype. Each prototype has its own figure of merit. The prototype with MF_{mi} is selected as the final prototype for a given mutation. MF_{mi} is the maximum value for the figure of merit for a given prototype.

Step 6, **Mutation to N points:** Mutate δ_k of prototype G using the following equation:

$$N_{n1} = \delta_{k0} + \tau \tag{3}$$

τ is the magnitude of mutation that is computed as:

$$\tau = \varepsilon \alpha \mu \tag{4}$$

ε is a random sign symbol, $\alpha \in [0,1]$, and μ is the maximum perturbation that is computed as:

$$\mu = \begin{cases} Mx + \delta_k, & \text{if } \delta_k > \dfrac{\text{Mx+Mn}}{2} \\ \delta_k, & \text{otherwise} \end{cases} \tag{5}$$

Mx and *Mn* are the maximum and minimum values in the training set, respectively. In equation (3), N_{n1} is the random points for first mutation and δ_{k0} is the centre of a potential prototype in mutation 0 that is chosen as:

$$\sum_{b=1}^{k-1} f_b < \varsigma \leq \sum_{b=1}^{k} f_b \quad (6)$$

ς is a random number $\in [0,1]$ and f_b is the normalized figure of merit computed as:

$$f_m = \frac{F_{mi}}{\sum_{mi=1}^{gm} F_{mi}} \quad (7)$$

gm is the total number of potential prototypes for a given mutation. The mutation process is continued until all points in the class set are trained using a potential prototype or when the maximum number of mutations (*MM*) is reached. There is *MG* number of generations for the training phase and for each generation there is *MM* mutation.

Step 7, **Comparison:** Repeat Steps 3 through 6 until all the training points are trained or when the maximum number of mutations, *MM*, is reached. Based on experimental results, *MM=20* provided good outcome for our dataset.

Step 8, Start new generation: If at least one point in the training set is not classified, then start a new generation and reset the mutation to mutation 0.

Step 9, **Stop condition:** Proceed to the classification step if all the points in the training set are classified or when the maximum generation, *MG*, is reached. Based on experimental results, *MG=20* provided good outcome for our dataset.

Step 10, **Object classification:** Classify each pixel in the image, γ_i, to its corresponding class using the saved prototypes. γ_i is considered as object point if it has minimum Euclidean distance within the zero-margin radius.

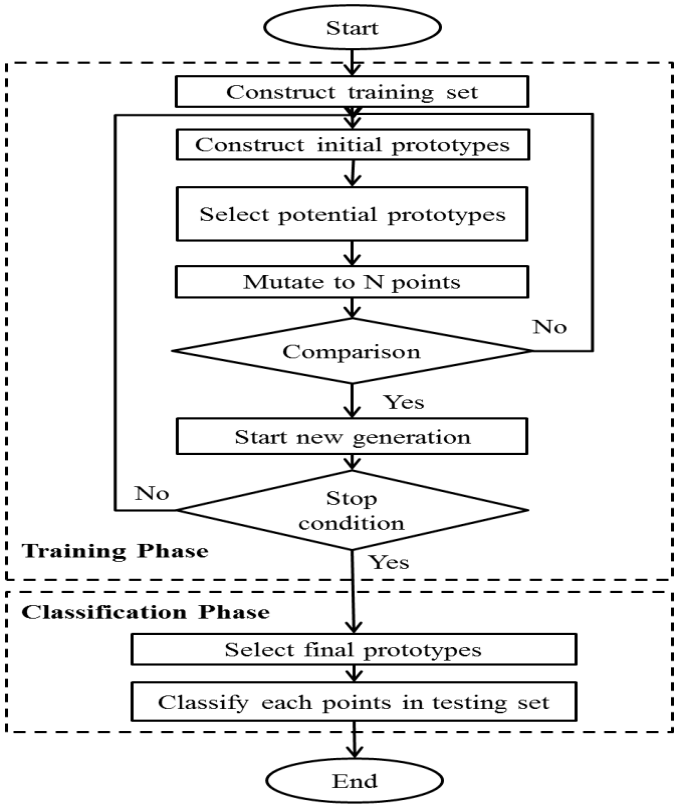

Figure 4. MSA flowchart

The output of the classification is then provided to a registration algorithm that uses the mutual information to measure the similarity between an image pair [20], [21]. This research was performed using a dataset which is explained in the next section.

2.3. Dataset

Segmentation algorithm is implemented on 554 mammograms for 125 patients. The mammograms are for craniocaudal (CC) and mediolateral oblique (MLO) views. The dataset is a private one provided by two radiologists who perform screening mammography in USA and Europe. The two radiologists provided the annotation for their datasets. All malignant cases are biopsy proven. Of the cases, 40 were of malignant nature: four cases have lesions of different shapes, seven with masses, eight with calcifications, three with architectural distortions, fourteen with asymmetric densities, and four with asymmetric densities and architectural distortions. The cancer free cases consists of 39 normal cases, three cases with masses, 41 cases with calcifications, one case with architectural distortion, and one case with asymmetric density. The dataset included two cases with implant. The density distribution for the cases is determined using BI-RADS classification. 36 of the mammograms are almost fatty, 26 are with scattered fibroglandular tissue, 45 are heterogeneously dense, and 18 are extremely dense.
The registration algorithm is applied to a subset of 28 cases which consists of temporal mammograms for the same patient over a period of time. The total number of the mammogram pairs is 76. Of these 28 cases, 15 were of malignant nature: three with masses, one with a lesion, three with calcifications, two with architectural distortion, four with asymmetric density, and two with asymmetric density and architectural distortions. Of the normal cases, one contains a mass, five with calcifications, and the rest are with normal tissues. The registration dataset included one case with implants. Six of the cases are almost fatty, five are with scattered fibroglandular tissue, 13 are heterogeneously dense, and four are extremely dense according to BI-RADS classification.

III. PROCEDURE, RESULTS, AND DISCUSSION

3.1 Segmentation Methodology

During the training phase of MSA algorithm, the decision boundaries are computed using intensity values. This requires selecting random pixels from the object and the background. The object is defined as the breast and the rest of the image information is considered as background. Experimenting with different number of pixels has shown that 20 points are sufficient to segment the object regardless of the non- uniformity of the object. As the background is more uniform, less number of pixels are needed. In the classification phase, the breast is classified using the computed decision boundaries. All the intensity values in the mammogram are the input for the classification phase. A post processing operation using a median filter of size 5x5 is used to remove impulse noise [27]. MSA performance is subjectively compared with NN and several thresholding algorithms; ACO, global, and Otsu [8], [17]-[19]. The input images for each algorithm are DICOM format of raw data and of size ~4000x3328. NN algorithm uses the same training and testing data points applied for MSA algorithm. For the thresholding techniques, high intensity values, 15% of the maximum intensity values for each mammogram, are removed to reduce the variation in the grayscale level and increase the accuracy of the segmentation step [30].
The segmentation results were evaluated subjectively by four experts in the area of pattern recognition using GUI software. GUI shows the segmented output images using different algorithms. The segmented images are positioned randomly with no title and are shown side by side on the same page. The order of segmented images is scrambled so they would not appear at the same position for different cases. The experts compared them with the original mammogram to determine which method provided better results.

3.2 Segmentation Evaluation

First, MSA is compared with ACO, global, and Otsu thresholding. The subjective evaluation for the MLO and CC views are shown in Table 1 and 2, respectively. Note that when at least two algorithms provided similar results the output was considered to be the same. Figure 5. shows the results of breast segmentation using the different thresholding techniques and MSA for four different mammograms.

Table 1. Subjective evaluation of breast segmentation in MLO view using four algorithms

Researcher\Algorithm	ACO	Global	MSA	Otsu	Same
Developer	0	0	268	0	16
Ph.D. Professor	17	6	254	3	4
Ph.D. Candidate 1	6	2	268	2	6
Ph.D. Candidate 2	2	1	273	0	8
Average	6	2	266	1	9

Table 2. Subjective evaluation of breast segmentation in CC view using four algorithms

Researcher\Algorithm	ACO	Global	MSA	Otsu	Same
Developer	0	0	257	0	13
Ph.D. Professor	0	0	258	1	11
Average	0	2	257	1	12

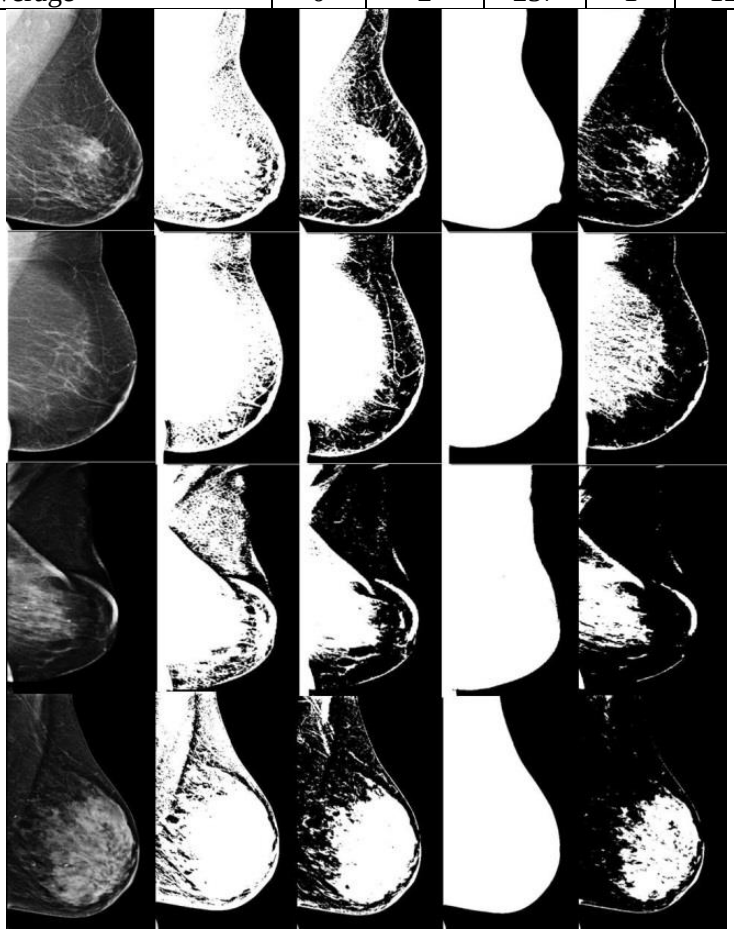

Figure 5. Breast detection, a) original mammogram, b) ACO, c) global, d) MSA, and e) Otsu thresholding, respectively

As the breast density decreases, Otsu and global thresholding failed to detect the fatty tissues within the parenchymal tissue. When the mammogram has gradual change in the grayscale level with no sharp edges that separate the background from the skin line, ACO failed to detect the skin line and the fatty region behind it. Figure 6. shows the detection rate for the three thresholding techniques in extremely dense breast. As shown in Figure 6., ACO detected the internal tissues but failed to detect the fatty region behind the skin line. Global thresholding detected the dense area but did not fully detect the fatty regions and Otsu only detected the dense regions [28].

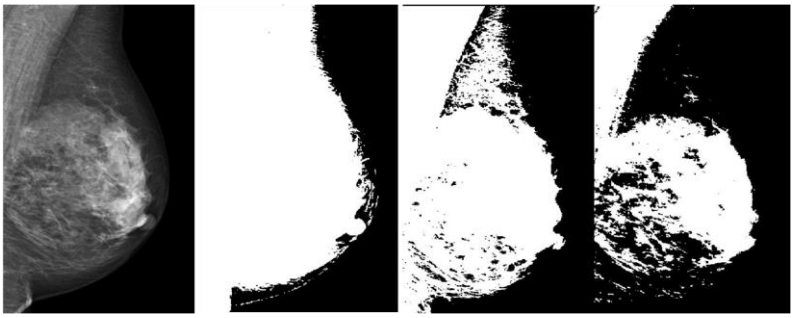

Figure 6. Breast segmentation using ACO, global, and Otsu thresholding, respectively

Subjective evaluation is also applied to compare the performance of MSA and NN algorithms in detecting the breast as shown in Table 3 and 4 for MLO and CC views, respectively.

Table 3. Subjective evaluation of breast segmentation in MLO view using MSA and NN

Researcher\Algorithm	MSA	NN	Same
Developer	77	15	192
Ph.D. Professor	65	31	188
Ph.D. Candidate 1	140	19	125
Average	94	22	168

Table 4. Subjective evaluation of breast segmentation in CC view using MSA and NN

Researcher\Algorithm	MSA	NN	Same
Developer	133	8	129
Ph.D. Professor	128	31	111
Average	130	20	120

Figures 7 and 8 show the breast segmentation using MSA and NN algorithms for three mammograms. NN detected the breast in most cases but did not provide a smooth skin line especially when the breast is not well separable from the background with no visible skin line. Also, it did not provide good detection for almost fatty breasts as seen in Figure 8. On the other hand, MSA detected the breast regardless of the breast type. Detection of the nipple when it is shown in the profile was also challenging for NN algorithm. MSA algorithm provided better results in detecting nipple even when it is with small intensity values that are so similar to the background. Figure 9. illustrates the difference between the two algorithms in detecting the nipple.

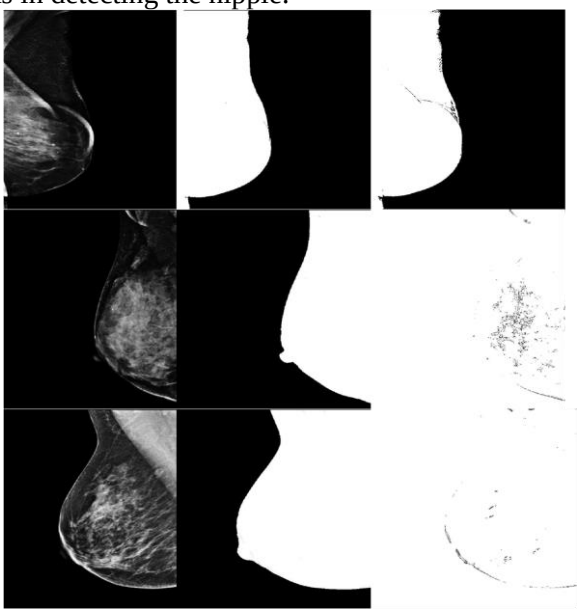

Figure 7. Breast detection for 3 mammograms, a) original, b) MSA, and c) NN, respectively, MLO view

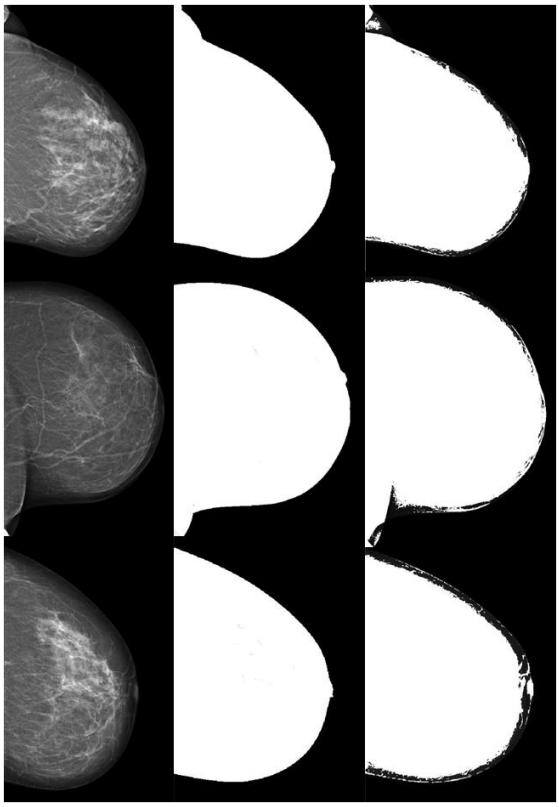

Figure 8. Breast detection for three mammograms, a) original mammogram, b) MSA, and c) NN, respectively, CC view

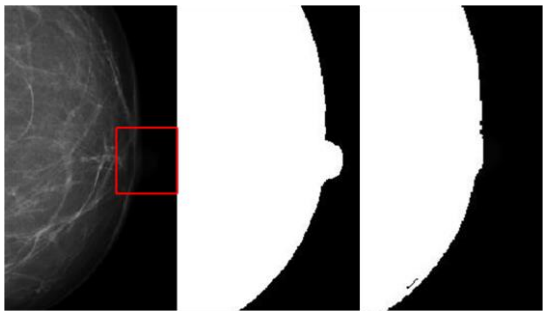

Figure 9. Comparing MSA and NN performance in detecting the nipple

3.3 Registration Methodology

The segmented mammograms are fed to the MI algorithm for registration [26]. Without loss of generality and to reduce the computational time the images are resized to 15% of the original size.

3.4 Registration Evaluation

Figure 10. shows the reference image and its segmented version using MSA algorithm. Figure 11. a) and b) show the target image and its segmented version using MSA. MI is applied to the target segmented mammogram. MI algorithm performs translation, rotation, scaling, and shearing on the target image to produce a registered target image of maximized mutual information with respect to the reference image [29]. Figure 11. c) displays the superimposed of the reference and target registered images.

The registration algorithm was evaluated objectively using signal to noise ratio (SNR) and correlation (CORR). The results are given in Table 5 where the average SNR and CORR values for 76 temporal images. Note that SNR are computed in db. In Table 5, a cell with (*_Original) value illustrates the SNR or CORR value between the reference and target images (with no registration). While, (*_Registered) value provides the SNR or CORR value between the reference and registered target images.

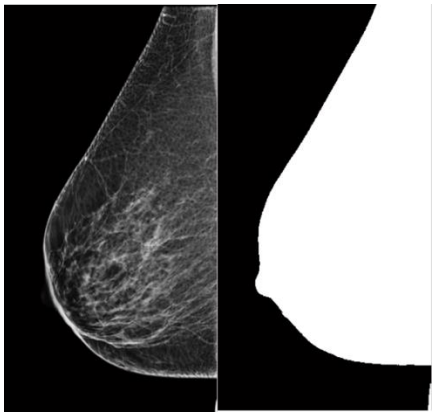

Figure 10. a) reference mammogram, and b) the segmented breast in a) using MSA

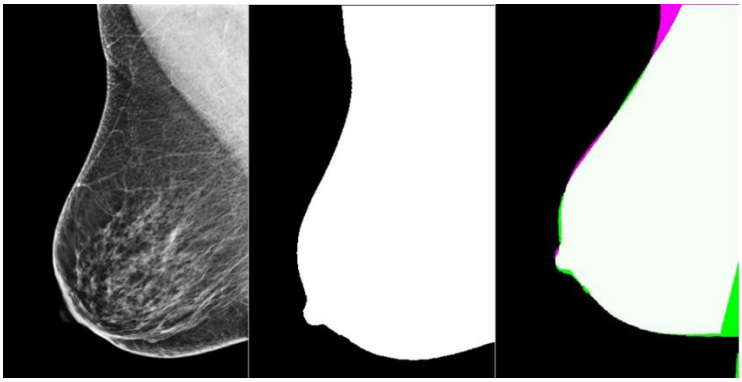

Figure 11. a) Target mammogram, b) segmented image of a), and c) superimposed reference and target images

Table 5. SNR and CORR for registration algorithms

Researcher\Metric Measurement	SNR	CORR
MSA_Original	7.39	0.83
MSA_Registered	9.32	0.87
Otsu_Original	1.01	0.53
Otsu_Registered	0.65	0.59
NN_Original	7.32	0.83
NN_Registered	9.30	0.86
ACO_Original	6.42	0.81
ACO_Registered	6.95	0.83

IV. CONCLUSIONS

MSA is designed for mammogram segmentation and registration. MSA uses prototypes to have a better classification for nonlinear patterns such as breasts in mammograms. MSA performance is compared with those of different thresholding techniques and NN using signal to noise ratio (SNR) and correlation (CORR). The (SNR, CORR) values for MSA is (9.32, 0.87). The computed (SNR, CORR) values for Otsu, NN, and ACO are (0.65, 0.59), (9.30, 0.86), and (6.95, 0.83), respectively. Considering these computed values, MSA outperforms the other thresholding techniques significantly. However, MSA provides a slight improvement over NN, namely (0.22%, 1.63%) for (SNR, CORR).

V. FUTURE WORK

Margin setting algorithm (MSA) is applied to separate the breast from the background in the mammographic images. MSA provided better results when compared to neural network (NN) and three thresholding algorithms. The current implement of MSA requires selecting training set from each mammogram. This needed to be replaced by a large number of training points from the entire

dataset. Another drawback is the use of normal distribution function to define the prototypes for different classes. This produces different outputs when the algorithm is run several times. Further research is necessary to increase the consistency and robustness of MSA outcome.

REFERENCES

[1] R. Martí, R. Zwiggelaar, R., and C. E. Rubin, C. E. Automatic Point Correspondence and Registration Based on Linear Structures. *International Journal Of Pattern Recognition & Artificial Intelligence*, *16*(3), 331, **2002**.
[2] W. Li, and H. Leung, A maximum likelihood approach for image registration using control point and intensity, *Image Processing, IEEE Transactions on* , vol.13, no.8, pp.1115-1127, August **2004**.
[3] M. Sonka, V. Hlavac, and R. Boyle, *Image Processing, Analysis, and Machine Vision*, Cengage learning, 4th edition, **2008**.
[4] F. Tavassoli, *Pathology of the Breast*, 2nd ed. Stamford, CT: Appleton & Lange, **1999**.
[5] D. Kopans, *Breast Imaging*, 2nd ed. Philadelphia, PA: Lippincott, Williams & Wilkins, **1998**.
[6] A. Sotiras, C. Davatzikos, and N. Paragios, Deformable Medical Image Registration: A Survey, *Medical Imaging, IEEE Transactions on* , vol.32, no.7, pp.1153-1190, July **2013**.
[7] L. C. Hartmann, and C. L. Loprinzi, *The Mayo Clinic Breast Cancer Book*, Good Books.
[8] R. C. Gonzalez, and R. E. Woods, *Digital Image Processing*, in Prentice Hall, 3rd edition, **2008**.
[9] J. Fu, H. J. Caulfield, and A. Bandyopadhyay, Pairing mathematical morphology with artificial color to extract targets from clutter, *Journal of Imaging Sci. and Tech.*, vol. 51, no. 2, pp.148-154, March **2007**.
[10] J. Fu, and H. J. Caulfield, Designing spectral sensitivity curves for use with artificial color, *Pattern Recognition*, vol. 40, issue 8, pp. 2251-2260, **2007**.
[11] J. Fu, H. J. Caulfield, D. Wu, and W. Tadesse, Hyperspectral image analysis using artificial color, *Journal of Applied Remote Sensing*, vol. 4, March **2010**.
[12] J. Fu, H. J. Caulfield, and C. Gelnn, Primitive attempt to turn images to percepts, *International Journal of Machine Learning and Cybernetics*, August **2013**.
[13] J. Fu, H. J. Caulfield, and T. Mizell, Applying median filtering with artificial color. *Journal Of Imaging Science And Technology*, *49*(5), 498-504.
[14] Y. Wang, R. Adhami, and J. Fu, A Novel Machine Learning Algorithm for Salt and Pepper Noise Removal, IEEE Conference, SSP, **2014**.
[15] H. J. Caulfield, F. Jian, and Y. Seong-Moo, Artificial color image logic. *Information Sciences*, *167*(1-4), 1-7, **2004**.
[16] H. J. Caulfield, A. Karavolos, and J. E. Ludman, Improving optical Fourier pattern recognition by accommodating the missing information, Information Sciences, in press.
[17] R. O. Duda, P. E. Hart, and D. G. Stork, *Pattern Classification*, in John Wiley & Sons, 2nd edition, **2001**.
[18] H. Al-Ghaib, and R. Adhami, On the Digital Image Additive White Gaussian Noise Estimation. IEEE International Conference on Industrial Automation and Information and Communications Technology (IAICT), pp.90-96, Bali, Indonesia, August **2014**.
[19] J. Tian, W. Yu, and L. Ma, Antshrink: Ant colony optimization for image shrinkage, *Pattern Recognit. Lett*., vol. 13, pp. 1751-1758, October **2010**.
[20] D. Loeckx, P. Slagmolen, F. Maes, D. Vandermeulen, and P. Suetens, P., Nonrigid Image Registration Using Conditional Mutual Information, *Medical Imaging, IEEE Transactions on* , vol.29, no.1, pp.19-29, January **2010**.
[21] D. Mattes, D. R. Haynor, H. Vesselle, T. Lewellen, and W. Eubank., Non-rigid multimodality image registration, *Medical Imaging: Image Processing SPIE Publications*, pp.1609–1620, 3 July **2001**.
[22] X. Zhao, M. Lee, and S. Kim, Improved Image Thresholding Using Ant Colony Optimization Algorithm, *Advanced Language Processing and Web Information Technology, ALPIT '08. International Conference on* , vol.210, no.215, pp.23-25. July **2008**.
[23] M. Hachama, A. Desolneux, and F. Richard, Bayesian Technique for Image Classifying Registration, *Image Processing, IEEE Transactions on* , vol.21, no.9, pp.4080-4091, September **2012**.
[24] J. M. Celaya-Padilla, J. Rodriguez-Rojas, V. Trevino, and J. Tamez-Pena, Local image registration a comparison for bilateral registration mammography, **2013.**
[25] A. Serifovic-Trbalic, D. Demirovic, D., and P. Cattin, Intensity-based hierarchical elastic registration using approximating splines. *International Journal Of Computer Assisted Radiology And Surgery*, vol.*9, no.*1, pp.21-27, **2014**.
[26] D. Rueckert, P. Aljabar, Nonrigid Registration of Medical Images: Theory, Methods, and Applications [Applications Corner], *Signal Processing Magazine, IEEE* , vol.27, no.4, pp.113,119, July **2010**.

[27] C. Zhili and R. Zwiggelaar, A combined method for automatic identification of the breast boundary in mammograms, *Biomedical Engineering and Informatics (BMEI), 2012 5th International Conference on* , vol., no., pp.121,125, 16-18 October **2012**.
[28] O. Faust, U. R. Acharya, and T. Tamura, Formal Design Methods for Reliable Computer-Aided Diagnosis: A Review, *Biomedical Engineering, IEEE Reviews in* , vol.5, no., pp.15-28, **2012**.
[29] G.Yujun, R. Sivaramakrishna, L. Cheng-Chang, J. S. Suri, and S. Laxminarayan, Breast image registration techniques: a survey, *Medical and Biological Engineering and Computing*, vol.44, no.1/2, pp.15-26, **2006**.
[30] O. J. Peart, *Mammography and Breast Imaging Prep: Program Review and Exam Prep*, 1st edition, McGraw-Hill Companies, Inc., **2012**.

AUTHORS BIOGRAPHY

Huda Al-Ghaib received her bachelor degree in computer engineering from the University of Technology in Baghdad-Iraq in 2006. She worked in the Ministry of Higher Education and Scientific Research from 2007-2009 as an engineer. Ms. Al-Ghaib was a recipient of a Fulbright Scholar in 2009 for which she earned her Masters' degree in electrical engineering in 2011 from the University of Alabama in Huntsville (UAH). Currently, she is pursuing her Ph.D. in electrical engineering at UAH. Her research findings have been published in more than 10 articles. Her research areas include digital signal processing and digital image processing with applications in medical field. Ms. Al-Ghaib was the recipient of outstanding graduate student of college of engineering in 2014. She is a member in IEEE.

Reza Adhami received the B.S.E., M.S.E, and Ph.D. degrees in electrical engineering from the University of Alabama, Huntsville (UAH), in 1980, 1981, and 1985, respectively. He has 35 years of academic and industrial experience. Dr. Adhami served as the Electrical and Computer Engineering Department Chair at the University of Alabama in Huntsville from 1997 to 2010 and Director of the shared Ph.D. program between the University of Alabama in Birmingham and UAH. Currently, he is an emeritus professor of Electrical and Computer Engineering at UAH. His research interests include medical image processing, VLSI, signal processing, applications of biometrics in information assurance. He has published two books and numerous journal and conference articles. Dr. Adhami has been recognized by different organizations for his contributions to high quality research, education, and leadership. He is a recipient of several national and regional awards including the IEEE USA Professional Achievement Award for "leadership in building collaborative relationships between industry and academia", IEEE Region III Outstanding Educator Award, and the Maurice Simpson Award for excellence in technical publication.

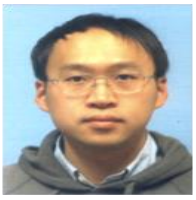

Yi Wang received his B.S. degree in Information Management and Information System from Wuhan University of Science and Technology, Wuhan, China, in 2006, and M.S. degree in Computer Science from the same university in 2009. He is currently pursuing his Ph.D. degree in Computer Engineering from UAH. His research interests are image processing and pattern recognition.